

# Candidate coronal mass ejection heating mechanisms

N. A. Murphy, J. C. Raymond, & K. E. Korreck  
 Harvard-Smithsonian Center for Astrophysics, Cambridge, MA

## Abstract

Several recent observational results suggest that coronal mass ejection (CME) plasma is heated even after leaving the flare site. The source of this heating is probably the magnetic field, but the mechanisms that convert magnetic to thermal energy during these events are not well understood. In the context of CMEs observed by SOHO/UVCS and analyzed using a time-dependent ionization code, we assess the efficacy of several candidate mechanisms, including heating by the CME current sheet, kink/tearing instabilities of the flux rope, turbulence, thermal conduction, energetic particles, and wave heating. Further tests of these models require investigating many events using a standardized method, so we discuss progress on automating this time-dependent ionization technique to constrain heating rates for a large number of CMEs.

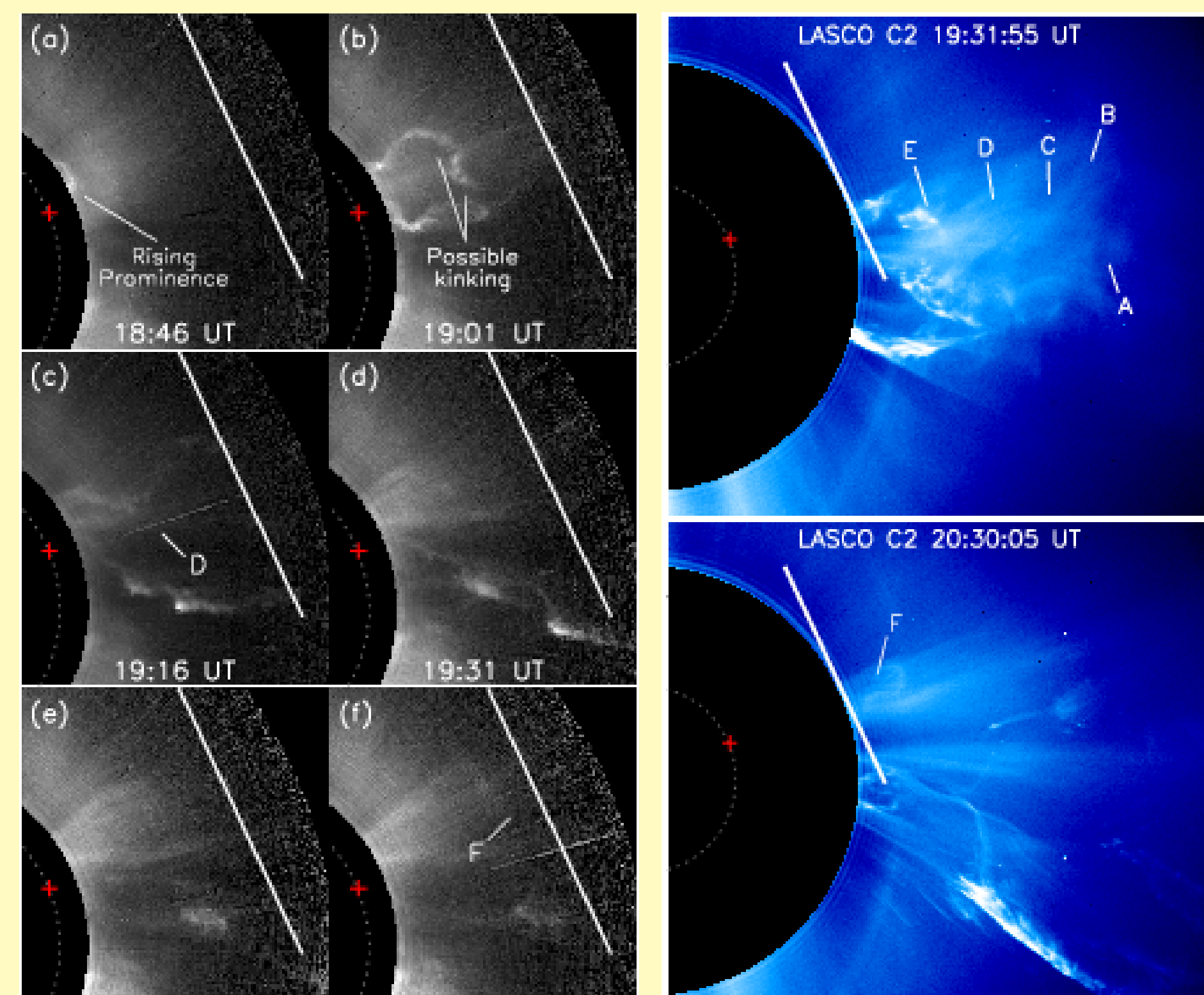
## Introduction

The energy budget of CMEs is an emerging area of research.

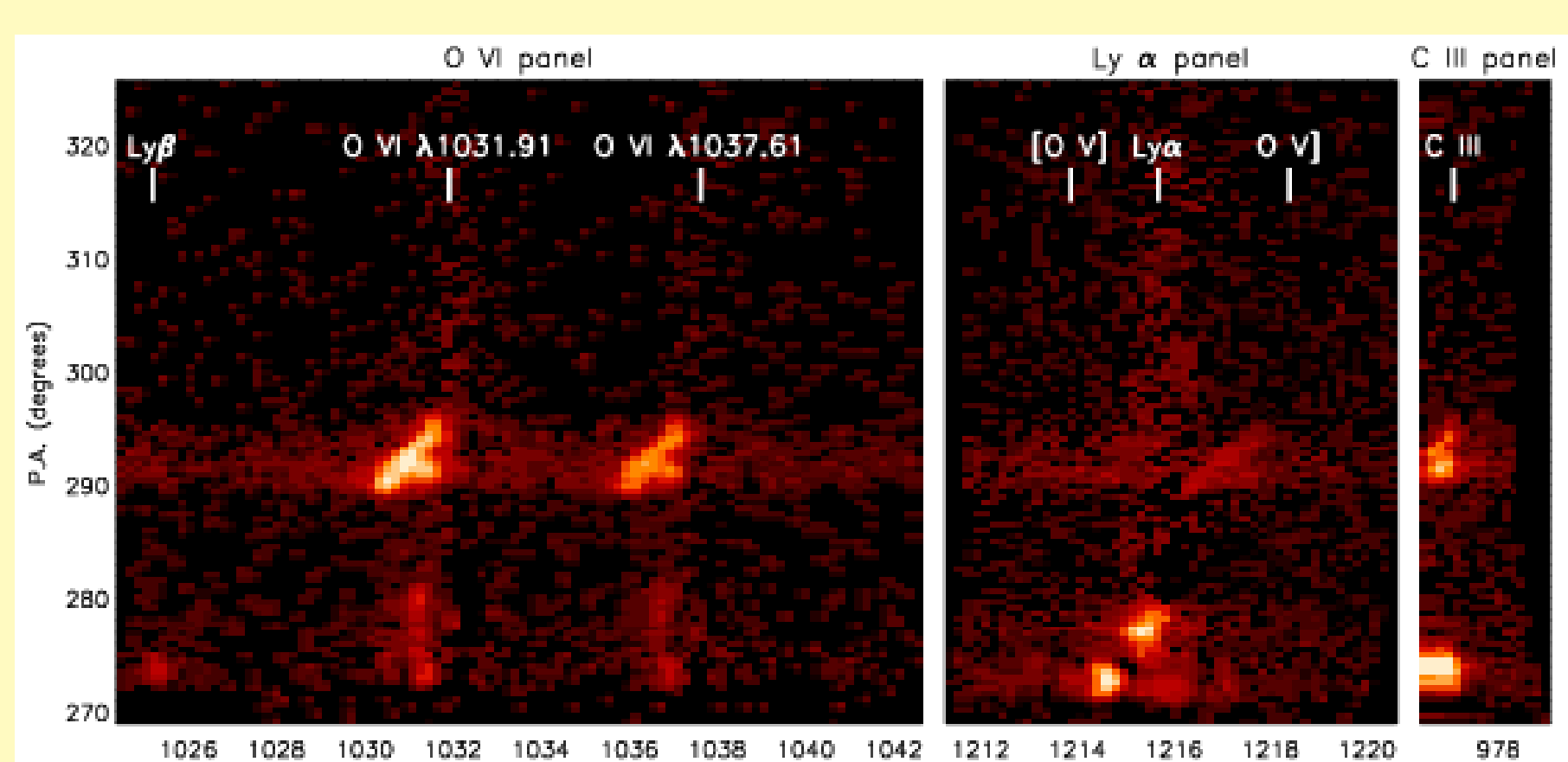
- While kinetic and potential energies are relatively straightforward, finding the heating rates and thermal energy content is more challenging.
- The Ultraviolet Coronagraph Spectrometer (UVCS) aboard the *Solar and Heliospheric Observatory* (SOHO) provides the opportunity to analyze the thermal component of the energy budget (e.g., Akmal et al. 2001; Lee et al. 2009; Landi et al. 2010).
- The ejected material is not in ionization equilibrium, so it is necessary to track the ionization states of the plasma from the flare site to the position observed by UVCS.
- Because of a lack of diagnostics, the magnetic energy is even more difficult to obtain than the thermal energy and heating rates.

## Observations

White light coronagraph observations were taken by MLSO/MK4 (left) and LASCO C2 and C3 (right) of a CME on 28 June 2000. The LASCO CME catalog gives a mass of  $\sim 7.3 \times 10^{15}$  g and an in-plane velocity of  $\sim 1200$  km/s for the leading edge.



Measurements with UVCS were taken with a two minute cadence throughout this event. The UVCS slit was positioned at P.A. =  $295^\circ$  at  $2.32 R_\odot$  above the northwest limb. Below are spectra taken at 20:12 UT. Shown is Blob F.



The density at the UVCS slit is found using one of two methods:

1. The ratio of the [O v]  $\lambda 1213$  forbidden line to the O v  $\lambda 1218$  intercombination line (Akmal et al. 2001)
2. Radiative pumping of the O vi  $\lambda\lambda 1032, 1038$  doublet chromospheric Ly  $\beta$ , O vi  $\lambda 1032$ , or C ii  $\lambda 1036$  (Noci et al. 1987; Raymond & Ciaravella 2004)

## Constraints on plasma heating

Constraints on plasma heating are found by comparing UVCS observations to a time-dependent ionization code (Akmal et al. 2001).

- Starting from a range of initial densities and temperatures and assuming homologous expansion, the code tracks ionization fractions until it reaches the UVCS slit.
- Several different heating parameterizations are used including an exponential wave heating model by Allen et al. (1998), heating proportional to  $n$  and  $n^2$ , and the model of Kumar & Rust (1996). The heating counters radiative losses and cooling by adiabatic expansion.
- The observed line ratios from the UVCS diagonal spectral feature are used as constraints for the model. We assume that the O v and O vi emission are from the same source and use the other line strengths as upper limits.
- The total heating consistent with UVCS observations for each blob are (in  $10^{14}$  ergs  $g^{-1}$ ):

Blob	exp.	$q \propto n$	$q \propto n^2$	KR
A	6.9–27	16.4–64	—	7.9–209
B	0.29–26	16.4–106	1330–3332	12–317
C	0.2–29	0.7–109	215–3403	3.6–314
D	0.1–21	0.5–75	230–3654	5.9–343
E	9.7	21	3897	15–34
F	12.7–31	22	—	85

- The kinetic and gravitational potential energies are estimated to be (in  $10^{14}$  erg  $g^{-1}$ ):

Blob	Kinetic	Gravitational
A	272 (>58)	7.4–7.8
B	328 (>53)	7.9–8.1
C	272 (>54)	7.7–8.1
D	272 (>38)	7.9–8.1
E	328 (>33)	8.2–8.3
F	17 (>11)	5.5–8.2

where the kinetic energies assume the velocity given by O vi pumping (lower limits in parentheses).

- The best constrained feature (Blob F) shows that the total heating required must be comparable to or greater than the kinetic energy of the feature.

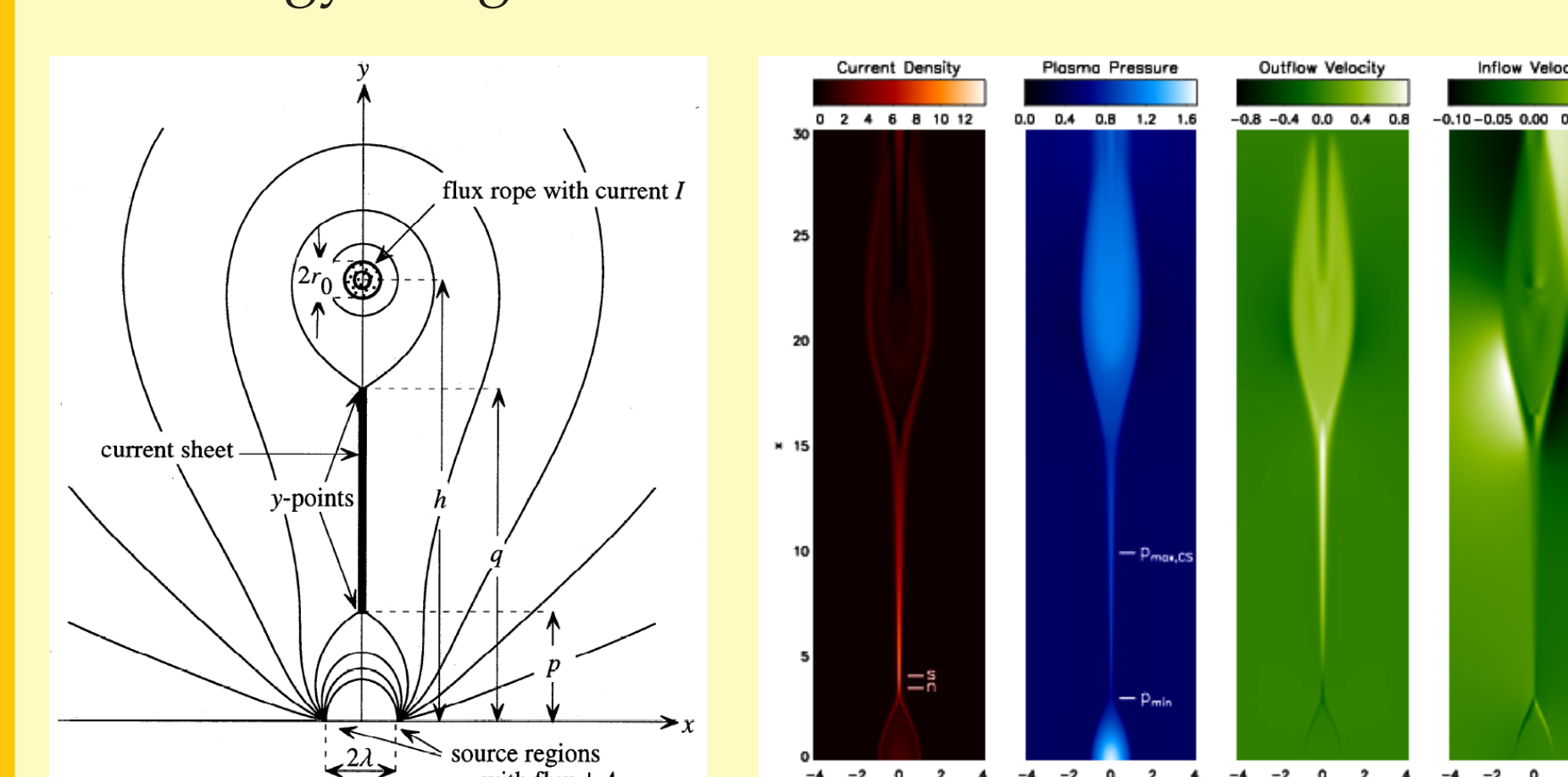
## Standardization of this analysis

This time-dependent ionization technique has been used to constrain heating during several events (Akmal et al. 2001; Ciaravella et al. 2001; Lee et al. 2009; Landi et al. 2010). The assumptions made for each of these events differ, thus complicating comparisons between events. To enable straightforward comparisons, we are implementing a standardized method which we will apply to  $\sim 10$ –20 events.

1. Identify candidate CMEs observed by UVCS.
2. Run a script to find features with good O v or O vi density diagnostics.
3. Run a script to find line strengths for these features.
4. Use white light observations to identify these features, find velocity curves, and column densities.
5. When possible, use EIT and other observations to provide further constraints.

## Heating by the Current Sheet

Most models of CMEs predict that a current sheet develops behind the rising flux rope (e.g., Lin & Forbes 2000). CME current sheets might contribute substantially to the mass and energy budgets of these events.



Recent simulations suggest that most of the outflow energy is directed upward towards the rising flux rope (e.g., Reeves et al. 2010; Murphy 2010). Reconnection heating cannot be parameterized in a 1-D model. Constraints on this heating mechanism require comparing observations to time-dependent ionization analyses of MHD simulations.

## Additional heating mechanisms

There are several candidate mechanisms which may dissipate magnetic energy into thermal energy during CMEs.

- Wave heating by photospheric motions have been ruled unlikely for a different event (Landi et al. 2010), but waves generated by the eruption itself could deposit energy into the surrounding medium (e.g., Tripathi & Gekelman 2010).
- A weak C3.7 flare was associated with this large and powerful CME. This suggests that flare energy was insufficient to heat the ejecta through energetic particles or thermal conduction, but the flare may have been partially occulted by the solar limb.
- Kink-like motions were observed by MLSO around 19:00 UT. These motions can drive turbulent motions which dissipate to heat the plasma. However, since the motions were slow compared to the propagation speed, we consider this mechanism unlikely to provide sufficient heating.
- Dissipation of turbulence is a likely intermediate step for most of these candidate mechanisms. The O vi line widths are  $\Delta V_{1/e} \approx 100$  km  $s^{-1}$  for the diagonal feature observed by UVCS (Blob F). This puts an upper limit on the turbulent energy density of  $U_{\text{turb}}/\rho \lesssim \Delta V_{1/e} \approx 10^{14}$  ergs  $g^{-1}$ . Because  $U_{\text{turb}}/\rho$  is much less than the total heating required, we conclude that turbulence must be continually injected into the system and dissipated on time scales much shorter than a propagation time for this to be a viable component of heating models.
- Filippov & Koutchmy (2002) describe a heating mechanism for prominences where upward concave flux rope segments lead to shocks from colliding flows. However, there is insufficient gravitational energy available to account for the inferred heating.
- An additional consideration to be addressed in future work is the effect of a non-Maxwellian population of energetic particles. Hot particles can increase ionization rates but can also heat the plasma.
- Analogous heating mechanisms probably occur in laboratory plasmas (e.g., Tripathi & Gekelman 2010). Relevant devices include RSX at LANL, MRX at PPPL, LAPD at UCLA, and the Caltech spheromak experiment.

## Conclusions

- The total heating of CMEs is comparable to or greater than the kinetic energy of the ejecta, and is an important term in the CME energy budget.
- Candidate heating mechanisms include upflow from the CME current sheet, wave heating, energetic particles, thermal conduction, large-scale MHD instabilities, dissipation of turbulence, and small-scale reconnection in the rising flux rope.
- Observations of the 28 June 2000 CME suggest that heating via the kink instability, thermal conduction, colliding flows, and energetic particles are unlikely to be significant.
- To better understand CME heating, we will perform a standardized version of this analysis for  $\sim 10$ –20 events.

## References

- [1] Akmal, A., Raymond, J. C., Vourlidas, A., Thompson, B., Ciaravella, A., Ko, Y.-K., Uzzo, M., & Wu, R. 2001, ApJ, 553, 922
- [2] Allen, L. A., Habbal, S. R., & Hu, Y. Q. 1998, J. Geophys. Res., 103, 6551
- [3] Ciaravella, A., Raymond, J. C., Reale, F., Strachan, L., & Peres, G. 2001, ApJ, 557, 351
- [4] Filippov, B., & Koutchmy, S. 2002, Sol. Phys., 208, 283
- [5] Kumar, A., & Rust, D. M. 1996, J. Geophys. Res., 101, 15667
- [6] Landi, E., Raymond, J. C., Miralles, M. P., & Hara, H. 2010, ApJ, 711, 75
- [7] Lee, J.-Y., Raymond, J. C., Ko, Y.-K., & Kim, K.-S. 2009, ApJ, 692, 1271
- [8] Lin, J., & Forbes, T. G. 2000, J. Geophys. Res., 105, 2375
- [9] Murphy, N. A. 2010, Phys. Plasmas, 17, 112310
- [10] Noci, G., Kohl, J. L., & Withbroe, G. L. 1987, ApJ, 315, 706
- [11] Raymond, J. C., & Ciaravella, A. 2004, ApJL, 606, L159
- [12] Reeves, K. K., Linker, J. A., Mikić, Z., & Forbes, T. G. 2010, ApJ, 721, 1547
- [13] Tripathi, S. K. P., & Gekelman, W. 2010, PRL, 105, 075005

## Acknowledgements

The authors thank M. P. Miralles, J.-Y. Lee, G. Attrill, E. Zweibel, S. Cranmer, T. Forbes, and E. Robbrecht for advice and assistance. This research is supported by NASA Grant NNX09AB17G.